

**$\theta$ -dependence of light nuclei and nucleosynthesis**Dean Lee<sup>1,\*</sup>, Ulf-G. Meißner<sup>2,3,4,†</sup>, Keith A. Olive<sup>5,‡</sup>, Mikhail Shifman<sup>5,§</sup> and Thomas Vonk<sup>2,||</sup><sup>1</sup>Facility for Rare Isotope Beams and Department of Physics and Astronomy, Michigan State University, Michigan 48824, USA<sup>2</sup>Helmholtz-Institut für Strahlen- und Kernphysik and Bethe Center for Theoretical Physics, Universität Bonn, D-53115 Bonn, Germany<sup>3</sup>Institute for Advanced Simulation, Institut für Kernphysik, and Jülich Center for Hadron Physics, Forschungszentrum Jülich, D-52425 Jülich, Germany<sup>4</sup>Tbilisi State University, 0186 Tbilisi, Georgia<sup>5</sup>William I. Fine Theoretical Physics Institute, School of Physics and Astronomy, University of Minnesota, Minneapolis, Minnesota 55455, USA

(Received 26 June 2020; accepted 18 August 2020; published 10 September 2020)

We investigate the impact of the QCD vacuum at nonzero  $\theta$  on the properties of light nuclei, Big Bang nucleosynthesis, and stellar nucleosynthesis. Our analysis starts with a calculation of the  $\theta$ -dependence of the neutron-proton mass difference and neutron decay using chiral perturbation theory. We then discuss the  $\theta$ -dependence of the nucleon-nucleon interaction using a one-boson-exchange model and compute the properties of the two-nucleon system. Using the universal properties of four-component fermions at large scattering length, we then deduce the binding energies of the three-nucleon and four-nucleon systems. Based on these results, we discuss the implications for primordial abundances of light nuclei, the production of nuclei in stellar environments, and implications for an anthropic view of the universe.

DOI: [10.1103/PhysRevResearch.2.033392](https://doi.org/10.1103/PhysRevResearch.2.033392)**I. INTRODUCTION**

One of the most outstanding questions in physics pertains to the values of the fundamental parameters in the Standard model. These include the gauge and Yukawa couplings, the latter being responsible for fermion masses and mixings. In the case of the gauge couplings, some hint is available from grand unified theories where a single unified coupling is run down from a very high energy scale to the weak scale leading to predictions for the weak scale gauge couplings in reasonable agreement with experiment. The Yukawa coupling matrices are, however, a bigger mystery which includes the generation structure of fermion masses. The answer may lie in an as yet undefined future theory (e.g., a complete string theory) in which case there is hope of a deeper understanding. It is also possible that our Universe with its observed fundamental parameters is part of a larger structure or a *Multiverse*, but we have no means to know. In this case, the observed values, may be somewhat random with no deep explanation. However, even in that case, our specific measurements of these parameters can not be completely random, as not all

values will permit a Universe which supports our form of life, which can carry out such measurements. This is often referred to as the anthropic principle. The anthropic principle absolves us, the Earth dwellers, from the duty of explaining the values of the governing constants, at least for the time being, until data at higher scales become available.

The term anthropic principle was coined in 1974 by Brandon Carter [1]. In the 1980s a few influential “anthropic papers” were published by Steven Weinberg, see, e.g., Ref. [2] (see also Refs. [3,4]). The anthropic principle is not a predictive theory, rather it is a philosophical idea that the governing parameters in our world should fit the intervals compatible with the existence of conscious life. The recent LHC data show no signs to support an opposite philosophical principle—that of *naturalness*.

The most remarkable and still incomprehensible example of anti-naturalness is the cosmological constant (for a different view, see e.g. [5]). Its observed value is suppressed by 124 orders of magnitude compared to the Planck scale  $M_P^4$  (believed to be the only fundamental scale). The suppression of the electroweak scale compared to  $M_P$  is 17 orders of magnitude. The vacuum angle  $\theta$ , whose natural order of magnitude  $\sim 1$  is less than  $10^{-10}$  in experiment [6].

It is obvious that the suppression of the cosmological constant is vital for the existence of our world. Even if it were a few orders of magnitude larger, the Universe would have entered an inflationary stage before the onset of galaxy formation. The smallness of the  $u, d$  quark masses compared to  $\Lambda_{\text{QCD}}$  and the fact that  $m_u < m_d$  are crucial for the genesis of heavier elements in stars. However, it is widely believed that there are no anthropic limitations on  $\theta$  and its suppression *must* be solved through a natural mechanism such as a symmetry including axions [7,8]. A dedicated study of this issue [9]

\*leed@frib.msu.edu

†meissner@hiskp.uni-bonn.de

‡olive@umn.edu

§shifman@umn.edu

||vonk@hiskp.uni-bonn.de

revealed some  $\theta$ -dependence on nuclear physics but the author concludes with the statement that “these effects are not too dramatic.” The authors of [7] note with regards to the vacuum angle  $\theta$  that it “is hard to see an anthropic argument that  $\theta$  [...] is bounded by  $10^{-10}$ . Moreover, in the flux vacua, there is typically no light axion.” For further discussions related to this issue, see Refs. [10–12]. In the present paper we revisit this issue.

While it is certainly true (and will be made clear below) that  $\theta \sim 10^{-9}$  or even  $\theta \sim 10^{-5}$  will not change life in our world, it seems reasonable to reconsider constraints imposed on  $\theta$  from observations other than the neutron electric dipole moment (nEDM) as well as the anthropic perspective. We will see that the impact of  $\theta$  on delicate aspects of nuclear physics is similar to that of the parameters  $|m_u|$  or  $|m_d|$ . Quark mass variation of nuclear properties and reactions are considered, e.g., in Refs. [13–26]. Furthermore, if the variation of quark masses is due to an overall variation in the Yukawa couplings, it will feed into variations of a host of fundamental observables including the gauge couplings, and affect Big Bang Nucleosynthesis (BBN) [27–31], the lifetime of long-lived nuclei [32], and atomic clocks [33]. Strictly speaking, it would be more appropriate to combine the absolute values of the quark masses with their phases and analyze the limitations in the complex plane. Here, we will fix  $|m_u|$  and  $|m_d|$  and let  $\theta$  vary. Unlike Ubaldi [9] who focused on CP-odd vertices and arrived at rather weak constraints, we will consider the  $\theta$ -dependence due to CP-even vertices. For reviews on this and related issues, see, e.g., Refs. [34–38].

Our approach is limited in the sense that we do not vary all governing parameters simultaneously in a concerted way. We do not explore how variations of some of them could be masked by variation of others, for instance whether the change of  $\theta$  could be compensated by that of  $|m_{u,d}|$  or the impact of  $\theta$  on, say, the vacuum energy density. Such a global task is a problem for the future. We will only vary  $\theta$  fixing all other parameters to their observed values.

At this point, it is worth noting that the most often discussed physical effect of  $\theta$  on an observable, the nEDM arising from strong CP-violation, does not impose strong anthropic constraints on  $\theta$ . The nEDM stemming from the QCD  $\theta$ -term is [39,40]

$$d_n(\bar{\theta}) = \mathcal{O}(10^{-16} \bar{\theta} e \text{ cm}), \quad (1.1)$$

where  $\bar{\theta} = \theta + \text{Arg det } \mathcal{M}$  and  $\mathcal{M}$  the quark mass matrix. Even if  $\theta = \mathcal{O}(1)$ , this is still a very small number and the physical effects of an nEDM of  $\mathcal{O}(10^{-16} e \text{ cm})$  on the evolution of the universe would still be negligible.

Note also that  $\theta = \pi$  is a special point in which QCD has two degenerate vacua, and physics changes drastically, see, e.g., the lucid discussion in Ref. [41] (and references therein). However, here we are not interested in this special point but rather in a generic situation with  $0 < \theta < \pi$ .

As we discuss below, the value of  $\theta$  does affect a host of hadronic properties which trigger changes in nuclear properties such as the binding energies of nuclei. Changes in  $\theta$  affect the pion mass which in turn alters the neutron-proton mass difference,  $\Delta m_N$  which further affects the neutron decay width. We also consider the effect of  $\theta$  on multi-nucleon systems and compute changes to nuclear binding energies.

The neutron-proton mass difference and the binding energy of deuteron,  $B_d$ , play a sensitive role in BBN (see Ref. [42] for the current status). As a result, changes in  $\theta$  can substantially alter the abundances of the light elements produced in BBN. Thus we can set limits on  $\theta$  (though they are weak) entirely independent of the nEDM. However, even with large changes in  $\theta$  and large changes in the light element abundances, it is not clear that this would cause an impediment on the formation of life in the Universe. Indeed, in a related study, Steigman and Scherrer [43] addressed the question of fine-tuning in the matter-antimatter asymmetry, as measured in terms of the baryon-to-photon asymmetry  $\eta_B$ . While the baryon asymmetry is reliant on the existence of CP violation [44], there is no reason to suspect that the baryon asymmetry is itself related to  $\theta$ . The authors of Ref. [45] found that even for  $\theta \sim 1$  the observed baryon asymmetry of the universe would not be altered. Nevertheless, changes in  $\eta_B$  strongly affect the light element abundances, though it was concluded by Steigman and Scherrer that these could not be excluded by anthropic arguments. A similar conclusion was reached in [46] considering the effects of altered weak interactions on BBN. Here, we fix  $\eta_B$  and consider the changes in abundances due changes in  $\Delta m_N$  and  $B_d$ .

The  $\theta$  induced changes will also affect stellar evolution and can lead to very different patterns of chemical evolution. In particular the changes in the nucleon-nucleon interaction, can lead to stars which yield little or no carbon or oxygen, thus potentially greatly affecting the existence of life in the Universe.

The manuscript is organized as follows: In Sec. II, we discuss the properties of various mesons and the nucleons at nonzero  $\theta$ . First, we collect the knowledge about the  $\theta$ -dependence of the corresponding hadron masses and coupling constants. Next, we focus on the modification of the neutron-proton mass difference and the neutron decay width. Then, we turn to the two-nucleon system in Sec. III. We first construct a simple one-boson-exchange (OBE) model to describe the two-nucleon system and then display results for the deuteron, the dineutron and the diproton with varying  $\theta$ . In Sec. IV A, we combine Wigner’s SU(4) symmetry with results from the literature to get a handle on the  $\theta$ -dependence of the three- and four-nucleon systems. Larger nuclei are briefly discussed in Sec. IV B. Implications of these results on the nucleosynthesis in the Big Bang and in stars are discussed in Secs. V and VI, respectively. We end with a summary and a discussion of our anthropic view of the universe in Sec. VII. The Appendix contains a derivation of the neutron-proton mass difference with varying  $\theta$ .

## II. ONE NUCLEON

In this section, we first collect the  $\theta$ -dependence of the various hadrons entering our study, i.e., of the pion, the  $\sigma$ ,  $\rho$  and  $\omega$  mesons as well as the nucleon mass. Our framework is chiral perturbation theory, in which the  $\theta$ -dependence of the nucleon (and also of the light nuclei) is driven by the  $\theta$ -dependence of the pion properties as well as the heavier mesons, which model the intermediate and short-range part of the nucleon-nucleon interaction. Of particular interest are the

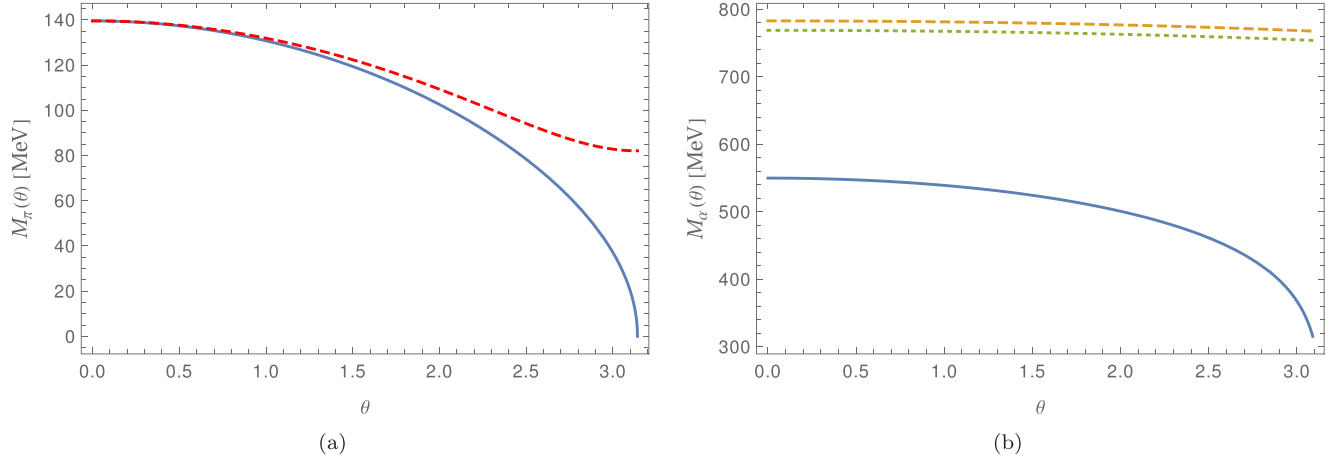


FIG. 1. The  $\theta$ -dependence of the various meson masses  $M_\alpha$  for  $\alpha = \{\pi, \sigma, \rho, \omega\}$ . (a) The  $\theta$ -dependence of the pion in the case of two degenerate flavors (blue solid line), and in the case with  $m_u \neq m_d$  (red dashed line). (b) The  $\sigma$  meson (blue solid line),  $\rho$  meson (green dotted line), and  $\omega$  meson (orange dashed line) masses as a function of  $\theta$ .

neutron-proton mass difference and the neutron decay width, which play an important role in BBN.

**A.  $\theta$ -dependence of hadron properties**

Consider first the pion mass. We use the leading order (LO)  $\theta$ -dependence for two flavors [47,48]<sup>1</sup>,

$$M_\pi^2(\theta) = M_\pi^2 \cos \frac{\theta}{2} \sqrt{1 + \varepsilon^2 \tan^2 \frac{\theta}{2}}, \quad (2.1)$$

with  $M_\pi = 139.57$  MeV, the charged pion mass, and  $\varepsilon = (m_d - m_u)/(m_d + m_u)$  measures the departure from the isospin limit. For two degenerate flavors, this reduces to

$$M_\pi^2(\theta) = M_\pi^2 \cos \frac{\theta}{2}. \quad (2.2)$$

A plot of both Eqs. (2.1) and (2.2) is shown in Fig. 1(a). Since the LO contribution gives about 95% [50] of the pion mass at  $\theta = 0$ , we do not need to consider higher order terms, as done e.g. in Ref. [51]. The impact of the isospin breaking term shows up mostly as  $\theta \rightarrow \pi$ . Note that while  $\varepsilon \sim 1/3$ , isospin symmetry is only broken by a few percent in nature as  $(m_d - m_u)/\Lambda_{\text{QCD}} \ll 1$ . Here, we take  $m_u = 2.27$  MeV and  $m_d = 4.67$  MeV (this refers to the conventional  $\overline{\text{MS}}$  scheme taken at the scale  $\mu = 2$  GeV).

The mass of the  $\sigma$  as well as the masses of the  $\rho$  and  $\omega$  mesons when  $\theta$  is varied are needed for the OBE model and are taken from Ref. [51], assuming  $M_\omega(\theta)/M_\omega(0) = M_\rho(\theta)/M_\rho(0)$  [Fig. 1(b)].

We consider the nucleon mass in the  $\theta$  vacuum to leading one-loop order (third order in the chiral expansion), which is given by [48]<sup>2</sup>

$$m_N(\theta) = m_0 - 4c_1 M_\pi^2(\theta) - \frac{3g_A^2 M_\pi^3(\theta)}{32\pi F_\pi^2}, \quad (2.3)$$

where  $m_0 \simeq 865$  MeV [52] is the nucleon mass in the chiral limit,  $g_A = 1.27$  the axial-vector coupling constant,  $F_\pi = 92.2$  MeV the pion decay constant, and  $c_1 = -1.1$  GeV<sup>-1</sup> [53] is a low-energy constant (LEC) from the second order chiral pion-nucleon Lagrangian,  $\mathcal{L}_{\pi N}^{(2)}$ , see, e.g., the review [54]. The  $\theta$ -dependence of the nucleon mass is thus entirely given in terms of the pion mass, and one finds  $m_N(0) = 938.92$  MeV. We show the  $\theta$  dependence of the nucleon mass in Fig. 2(a).

Next, we discuss the  $\theta$ -dependence of the coupling constants. The  $\theta$ -dependence of the pion-nucleon coupling is related to the Goldberger-Treiman discrepancy [55]

$$g_{\pi NN}(\theta) = \frac{g_A m_N(\theta)}{F_\pi} \left( 1 - \frac{2M_\pi^2(\theta)\bar{d}_{18}}{g_A} \right), \quad (2.4)$$

where  $\bar{d}_{18} = -0.47$  GeV<sup>-2</sup> so that  $g_{\pi NN}^2(0)/(4\pi) = 13.7$ , which is in accordance with the most recent and precise value from Ref. [56].

As  $g_{\rho\pi\pi}$  shows very little variation with  $\theta$  [51], we can use universality relation  $g_{\rho\pi\pi} = g_{\rho NN}$  [57] and keep  $g_{\rho NN}$  as well as  $g_{\omega NN}$  fixed at their values at  $\theta = 0$  in what follows. Matters are different for the  $\sigma$ . Similar to Ubaldi [9], we employ the parametrization of Refs. [58,59]. Writing the scalar attractive piece of the nucleon-nucleon interaction as

$$H_{\text{contact}} = G_S(\bar{N}N)(\bar{N}N), \quad (2.5)$$

it is evident that

$$G_S = -\frac{g_{\sigma NN}^2}{M_\sigma^2}, \quad (2.6)$$

when translated to an OBE model (this corresponds to resonance saturation of the corresponding LECs, see Ref. [60]). The following dependence of  $G_S(\theta)$  emerges [9]:

$$G_S(\theta) = G_S(0) \left( 1.4 - 0.4 \frac{M_\pi^2(\theta)}{M_\pi^2} \right), \quad (2.7)$$

where we have normalized again to the value at  $\theta = 0$ . Using Eq. (2.6) together with the known  $\theta$ -dependence of  $M_\sigma$ , we

<sup>1</sup>An equivalent expression for the  $\theta$ -dependence of the pion mass was also derived in a model of gluon dynamics in Ref. [49].

<sup>2</sup>Higher orders could be included, but that would go beyond the accuracy of our calculation.

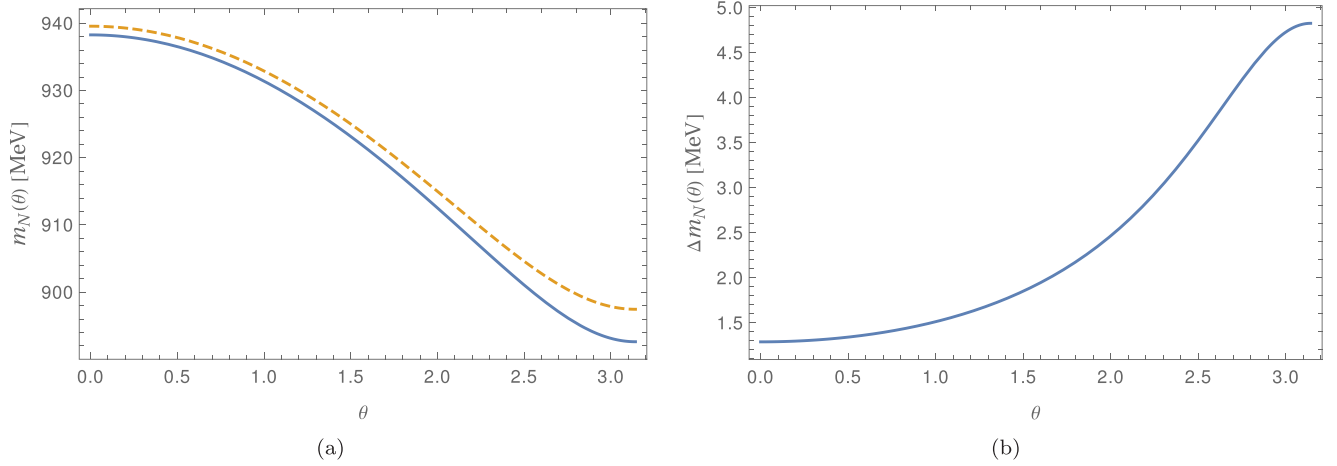


FIG. 2. The  $\theta$ -dependence of the nucleon masses  $m_N$ : (a) proton (blue solid line) and neutron (orange dashed line) and (b) neutron-proton mass difference.

can extract the variation of  $g_{\sigma NN}$  with  $\theta$ . We note that the coupling  $g_{\sigma\pi\pi}$  extracted from the work of Ref. [51] also decreases with  $\theta$ . We now have all of the pieces of the puzzle needed to calculate the binding energies of the various light nuclei. First, however, let us take a closer look at the neutron-proton mass difference and the neutron decay width, which also play an important role in BBN.

### B. Neutron-proton mass difference

Consider the neutron-proton mass difference

$$\Delta m_N = (m_n - m_p)^{\text{QED}} + (m_n - m_p)^{\text{QCD}} \simeq 1.29 \text{ MeV}. \quad (2.8)$$

The leading contribution to the strong part to the neutron-proton mass difference arises from the second order effective pion-nucleon Lagrangian and is given by [61]

$$\begin{aligned} (m_n - m_p)^{\text{QCD}} &= 4 c_5 B_0 (m_u - m_d) + \mathcal{O}(M_\pi^4) \\ &= -4 c_5 M_\pi^2 \varepsilon + \mathcal{O}(M_\pi^4), \end{aligned} \quad (2.9)$$

where  $c_5$  is a LEC. Using the most recent determination of the electromagnetic part of this mass difference,  $(m_n - m_p)^{\text{QED}} = -(0.58 \pm 0.16) \text{ MeV}$  [62], this amounts to  $(m_n - m_p)^{\text{QCD}} = 1.87 \mp 0.16 \text{ MeV}$  and correspondingly,  $c_5 = (-0.074 \pm 0.006) \text{ GeV}^{-1}$ . In the  $\theta$ -vacuum, this term turns into [63] (for a derivation, see Appendix)

$$(m_n - m_p)^{\text{QCD}}(\theta) \simeq 4 c_5 B_0 \frac{M_\pi^2}{M_\pi^2(\theta)} (m_u - m_d), \quad (2.10)$$

i.e the strong part of the neutron-proton mass increases (in magnitude) with  $\theta$ , see Fig. 2(b). At  $\theta \simeq 0.25$ ,  $\Delta m_N(\theta)$  deviates already by about 1% from its real world value, and for the range of  $\theta = 1-2$ , we find  $\Delta m_N(\theta) = 1.51 - 2.47 \text{ MeV}$ , using Eq. (2.1) for  $M_\pi(\theta)$ .

### C. Neutron decay width

As we increase  $\theta$ , the neutron-proton mass difference,  $\Delta m_N(\theta)$ , becomes larger and results in a larger three-body phase space for neutron beta decay. This increase in the phase

space integral scales roughly as the neutron-proton mass difference to the fifth power and is dominant over any expected  $\theta$ -dependence in the axial vector coupling,  $g_A$ . The neutron beta decay width can be written as (for the moment, we explicitly display factors of Planck's constant  $\hbar$  and the speed of light  $c$ , otherwise we work in natural units,  $k_B = \hbar = c = 1$ )

$$\Gamma_n = \frac{m_e^5 c^4}{2\pi^3 \hbar^6} |\mathcal{M}|^2 f, \quad (2.11)$$

where  $m_e$  is the electron mass,  $\mathcal{M}$  is the weak matrix element, and  $f$  is the Fermi integral,

$$f = \int_0^{m_n - m_p - m_e} F(Z, T_e) p_e T_e (m_n - m_p - m_e - T_e)^2 dT_e, \quad (2.12)$$

where  $Z = 1$  is the proton charge,  $T_e$  is the electron kinetic energy,  $p_e$  is the electron momentum, and  $F(Z, T_e)$  is the Fermi function that takes into account Coulomb scattering [64]. In Fig. 3, we plot  $[\Gamma_n(\theta)/\Gamma_n(0)]^{1/5}$  versus  $\Delta m_N(\theta) - m_e$  showing the linear behavior as expected. In Fig. 4, the neutron mean life is shown as a function of  $\theta$ . We see that the lifetime drops off very quickly when  $\theta$  starts to deviate from the

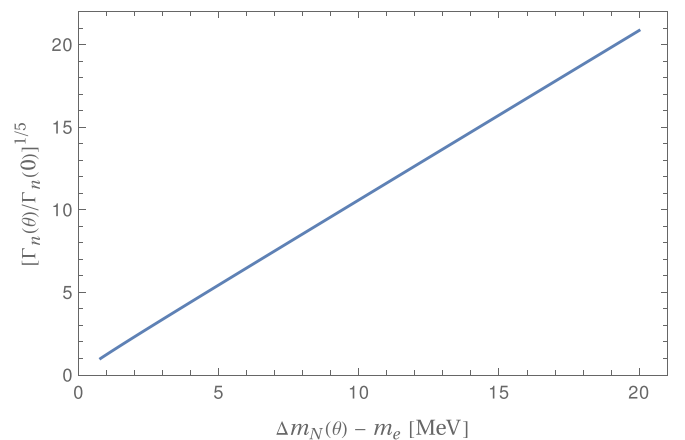


FIG. 3. Neutron decay width  $\Gamma_n(\theta)$  as a function of the neutron-proton mass difference. We plot the dimensionless quantity  $[\Gamma_n(\theta)/\Gamma_n(0)]^{1/5}$  vs  $\Delta m_N(\theta) - m_e$ .

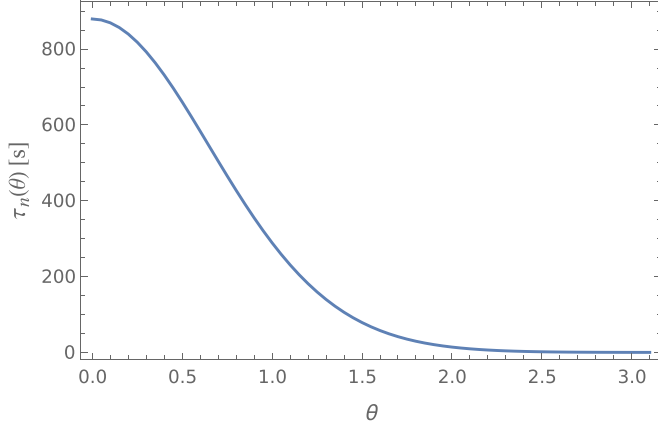


FIG. 4. Neutron life time  $\tau_n(\theta)$  as a function of  $\theta$ .

Standard model value  $\theta \approx 0$ . As we will see this dependence plays a big role at the start of BBN.

### III. TWO NUCLEONS

Here, we outline the formalism underlying our study of the two-nucleon system. First, we construct a simple OBE model, that allows us to describe the binding energies of the deuteron and the unbound dineutron and diproton at  $\theta = 0$ . Then, we discuss how these two-nucleon systems change when  $\theta$  varies from 0 to  $\pi$ .

#### A. OBE model

Consider first the case  $\theta = 0$ . We set up an OBE model inspired by Ref. [65] and work with the Schrödinger equation, as the nucleons in the deuteron move with velocities  $v \ll c$ . The corresponding OBE potential is given by

$$V_{\text{OBE}}(\mathbf{q}) = \sum_{\alpha=\{\pi,\sigma,\omega,\rho\}} V_{\alpha}(\mathbf{q}) \quad (3.1)$$

where  $\mathbf{q}$  denotes the momentum transfer. The static limit is applied, i.e. the four-momentum transfer squared  $q^2 = (p' - p)^2 = -(\mathbf{p}' - \mathbf{p})^2 = -\mathbf{q}^2$ . Setting furthermore  $L = 0$ , i.e. focusing on the dominant S-wave and neglecting the small D-wave contribution, the respective potentials can be reduced to

$$V_{\pi}(\mathbf{q}) = -(\boldsymbol{\tau}_1 \cdot \boldsymbol{\tau}_2)(\boldsymbol{\sigma}_1 \cdot \boldsymbol{\sigma}_2) \frac{g_{\pi NN}^2}{\mathbf{q}^2 + M_{\pi}^2} \frac{\mathbf{q}^2}{12m_N^2}, \quad (3.2)$$

$$V_{\sigma}(\mathbf{q}, \mathbf{P}) = -\frac{g_{\sigma NN}^2}{\mathbf{q}^2 + M_{\sigma}^2} \left( 1 + \frac{\mathbf{q}^2}{8m_N^2} - \frac{\mathbf{P}^2}{2m_N^2} \right), \quad (3.3)$$

$$V_{\omega}(\mathbf{q}, \mathbf{P}) = \frac{g_{\omega NN}^2}{\mathbf{q}^2 + M_{\omega}^2} \left( 1 - \frac{\mathbf{q}^2}{2m_N^2} \left[ \frac{1}{4} + \frac{1}{3}(\boldsymbol{\sigma}_1 \cdot \boldsymbol{\sigma}_2) \right] + \frac{3\mathbf{P}^2}{2m_N^2} \right), \quad (3.4)$$

$$V_{\rho}(\mathbf{q}, \mathbf{P}) = (\boldsymbol{\tau}_1 \cdot \boldsymbol{\tau}_2) \frac{g_{\rho NN}^2}{\mathbf{q}^2 + M_{\rho}^2} \left( 1 - \frac{\mathbf{q}^2}{2m_N^2} \left[ \frac{1}{4} + \frac{g_{\text{T}}^{\rho}}{g_{\rho NN}} + \frac{1}{3} \left( 1 + \frac{g_{\text{T}}^{\rho}}{g_{\rho NN}} \right)^2 (\boldsymbol{\sigma}_1 \cdot \boldsymbol{\sigma}_2) \right] + \frac{3\mathbf{P}^2}{2m_N^2} \right), \quad (3.5)$$

where  $\mathbf{P} = (\mathbf{p}' + \mathbf{p})/2$ . Terms  $\propto (\mathbf{q} \times \mathbf{P})$ , which in coordinate space correspond to terms  $\propto \mathbf{L}$ , the angular momentum operator, and terms  $\propto S_{12}(\mathbf{q}) = 3(\boldsymbol{\sigma}_1 \cdot \mathbf{q})(\boldsymbol{\sigma}_2 \cdot \mathbf{q}) - (\boldsymbol{\sigma}_1 \cdot \boldsymbol{\sigma}_2)|\mathbf{q}|^2$ , have been omitted. The potentials depend on the total spin  $S$  of the two-nucleon system through the factor  $(\boldsymbol{\sigma}_1 \cdot \boldsymbol{\sigma}_2) = 2S(S + 1) - 3$  and on the total isospin  $I$  through the factor  $(\boldsymbol{\tau}_1 \cdot \boldsymbol{\tau}_2) = 2I(I + 1) - 3$ . Note also that we omit from the start the  $\omega NN$  tensor coupling as the corresponding coupling constant  $g_{\omega}^T$  is approximately zero, which is a good approximation, see, e.g., Refs. [65,66].

The corresponding potentials in coordinate space are of Yukawa-type and given by

$$V_{\pi}(r) = (\boldsymbol{\tau}_1 \cdot \boldsymbol{\tau}_2)(\boldsymbol{\sigma}_1 \cdot \boldsymbol{\sigma}_2) \frac{g_{\pi NN}^2}{4\pi} \frac{1}{12} \left( \frac{M_{\pi}}{m_N} \right)^2 \frac{e^{-M_{\pi}r}}{r}, \quad (3.6)$$

$$V_{\sigma}(r) = -\frac{g_{\sigma NN}^2}{4\pi} \left( 1 - \frac{1}{4} \left( \frac{M_{\sigma}}{m_N} \right)^2 \right) \frac{e^{-M_{\sigma}r}}{r}, \quad (3.7)$$

$$V_{\omega}(r) = \frac{g_{\omega NN}^2}{4\pi} \left( 1 + \frac{1}{2} \left( \frac{M_{\omega}}{m_N} \right)^2 \left[ 1 + \frac{1}{3}(\boldsymbol{\sigma}_1 \cdot \boldsymbol{\sigma}_2) \right] \right) \frac{e^{-M_{\omega}r}}{r}, \quad (3.8)$$

$$V_{\rho}(r) = (\boldsymbol{\tau}_1 \cdot \boldsymbol{\tau}_2) \frac{g_{\rho NN}^2}{4\pi} \left( 1 + \frac{1}{2} \left( \frac{M_{\rho}}{m_N} \right)^2 \left[ 1 + \frac{g_{\text{T}}^{\rho}}{g_{\rho NN}} + \frac{1}{3} \left( 1 + \frac{g_{\text{T}}^{\rho}}{g_{\rho NN}} \right)^2 (\boldsymbol{\sigma}_1 \cdot \boldsymbol{\sigma}_2) \right] \right) \frac{e^{-M_{\rho}r}}{r}. \quad (3.9)$$

The OBE potential requires regularization since it is ultraviolet-divergent. This can be most easily seen from the momentum-space representation, Eqs. (3.2)–(3.5), as these potentials grow quadratically with increasing momentum transfer. A standard regularization procedure in nuclear physics is to apply either a single vertex form factor controlled by the cutoff mass  $\Lambda$  for the total potential, or four individual form factors controlled by the cutoff masses  $\Lambda_{\alpha}$  for each meson exchange potential. Here, we are only interested in the binding energies of the nucleon-nucleon systems, therefore a single form factor is sufficient. The total OBE potential in the coordinate-space representation is then:

$$V_{\text{OBE}}(r) = \sum_{\alpha=\{\pi,\sigma,\omega,\rho\}} V_{\alpha}(r) + \frac{\Lambda}{4\pi} \frac{e^{-\Lambda r}}{r}. \quad (3.10)$$

At  $\theta = 0$ , the meson masses we use are

$$\begin{aligned} M_{\pi} &= 139.57 \text{ MeV}, & M_{\sigma} &= 550 \text{ MeV}, \\ M_{\omega} &= 783 \text{ MeV}, & M_{\rho} &= 769 \text{ MeV}. \end{aligned} \quad (3.11)$$

In order to assess the parameter dependence, we take two sets of parameters, cf. Ref. [65]:

$$\begin{aligned} \frac{g_{\sigma NN}^2}{4\pi} &= 14.17, & \frac{g_{\rho NN}^2}{4\pi} &= 0.80, & \frac{g_{\omega NN}^2}{4\pi} &= 20.0, \\ \Lambda &= 1.364 \text{ GeV}, \end{aligned} \quad (3.12)$$

which we call *parameter set I*, and

$$\begin{aligned} \frac{g_{\sigma NN}^2}{4\pi} &= 8.06, & \frac{g_{\rho NN}^2}{4\pi} &= 0.43, & \frac{g_{\omega NN}^2}{4\pi} &= 10.6, \\ \Lambda &= 2.039 \text{ GeV}, \end{aligned} \quad (3.13)$$

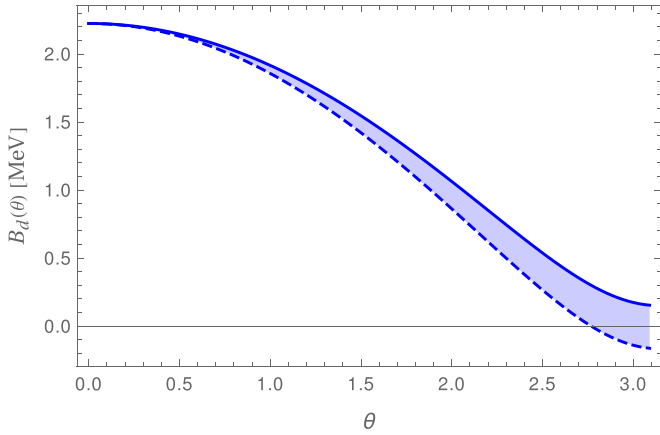


FIG. 5. The binding energy of the deuteron for a  $\theta$ -dependent OPE with all other meson couplings and masses are kept fixed, for parameter set I, Eq. (3.12) (solid line) and parameter set II, Eq. (3.13) (dashed line), respectively.

which we call *parameter set II*. For both sets, we take  $g_T^{\rho}/g_{\rho NN} = 6.1$  [65,66]. After solving the radial Schrödinger equation for the two nucleon system, one finds for both parameter sets a bound deuteron with binding energy  $E_d = -B_d = -2.224$  MeV, and an unbound dineutron with  $E_{nn} = -B_{nn} = 0.072$  MeV.

We now have all of the parts needed to investigate the  $\theta$ -dependence of the binding energies of the various two-nucleon systems.

### B. Spin-triplet channel

The bound state in the spin-triplet channel is the deuteron. Here, we work out the  $\theta$ -dependence of its binding energy.

Consider first the case of a  $\theta$ -dependent one-pion-exchange (OPE) potential, whereas all other potentials remain constant. The resulting  $\theta$ -dependent deuteron binding energy is shown in Fig. 5. If all OBE exchange potentials were independent of  $\theta$  except for the OPE potential, the deuteron's binding energy would slowly decrease until the deuteron would no longer be bound for  $\theta \gtrsim 2.8$  for parameter set II, Eq. (3.13). This is the expected behavior of the OPE potential that led to the idea that the deuteron for  $\theta \neq 0$  might not be bound anymore. This brief estimate demonstrates that the next-to-leading order contributions calculated by Ubaldi [9], which were reevaluated in Ref. [63], are (a) negligible (because they are CP-odd and only account for a shift of a few percent), but also that (b) the approach of applying first order perturbation theory is invalid, because the effects of  $\theta$  on the leading order OPE potential are not small.

However, the actual contribution of the OPE potential to the total OBE potential is very small, which can be seen, e.g., by considering the individual potentials  $V(r)$  of Eqs. (3.6)–(3.9). Clearly, the smallness of the OPE contribution compared to the strong repulsion of the  $\omega$  exchange potential and the large attraction of the  $\rho$  and  $\sigma$  exchange suggests that, even if the effects of  $\theta$  on the scalar and vector meson masses are not as pronounced as that for the pion, these contributions finally determine the actual  $\theta$ -dependence of  $B_d$ .

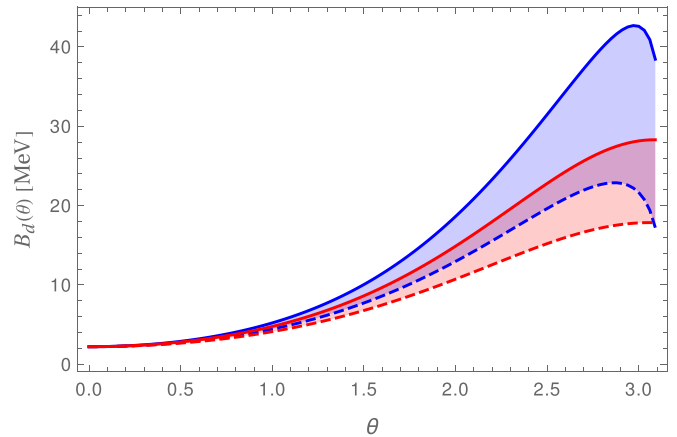


FIG. 6. The binding energy of the deuteron for the full  $\theta$ -dependent OBE model in the isospin symmetric case (blue upper band) and in the case of broken isospin symmetry (red lower band) for parameter set I, Eq. (3.12) (solid lines) and parameter set II, Eq. (3.13) (dashed lines), respectively.

Consider now the case of a full  $\theta$ -dependent OBE potential. We study two cases: first, the isospin symmetric case with  $m_u = m_d = (2.27 + 4.67)/2 = 3.47$  MeV, and second, the case of broken isospin symmetry with  $m_u = 2.27$  MeV and  $m_d = 4.67$  MeV. This gives the result shown in Fig. 6. In the isospin symmetric case, we find that after increasing and reaching a maximum at  $\theta \simeq 3.0$  (parameter set I, corresponding to  $B_d \simeq 42.5$  MeV) and  $\theta \simeq 2.9$  (parameter set II, corresponding to  $B_d \simeq 22.8$  MeV), respectively, the binding energy decreases and seems to approach to  $B_d$  in the chiral limit,  $B_d^{c.l.} \simeq F_\pi^2/m \simeq 10$  MeV [15], at least in the case of parameter set II. This behavior is expected: As we have set  $m_u = m_d$ ,  $\theta \rightarrow \pi$  effectively corresponds to  $m_u = m_d \rightarrow 0$ , since the charged and the neutral pion masses vanish in both cases. Because of that, all other phenomenological quantities such as the nucleon mass and the pion-nucleon coupling approach their respective values in the chiral limit.

In the case of broken isospin symmetry, the curve flattens and reaches its maximum as  $\theta \rightarrow \pi$ , which is given by  $B_d \simeq 28.3$  MeV (parameter set I) and  $B_d \simeq 17.8$  MeV (parameter set II). A useful analytic approximation for  $B_d(\theta)$  is given by

$$B_d(\theta) = 2.22 + c_1(1 - \cos \theta) + c_2(1 - \cos \theta)^2 + c_3(1 - \cos \theta)^3 \quad (3.14)$$

with

unbroken isospin symmetry:

$$\begin{cases} c_1 = 9.14 & c_2 = -7.19 & c_3 = 6.30 & \text{set I} \\ c_1 = 3.25 & c_2 = 2.55 & c_3 = 0.47 & \text{set II} \end{cases} \quad (3.15)$$

broken isospin symmetry:

$$\begin{cases} c_1 = 5.68 & c_2 = -1.02 & c_3 = 2.36 & \text{set I} \\ c_1 = 3.77 & c_2 = 0.45 & c_3 = 0.80 & \text{set II} \end{cases} \quad (3.16)$$

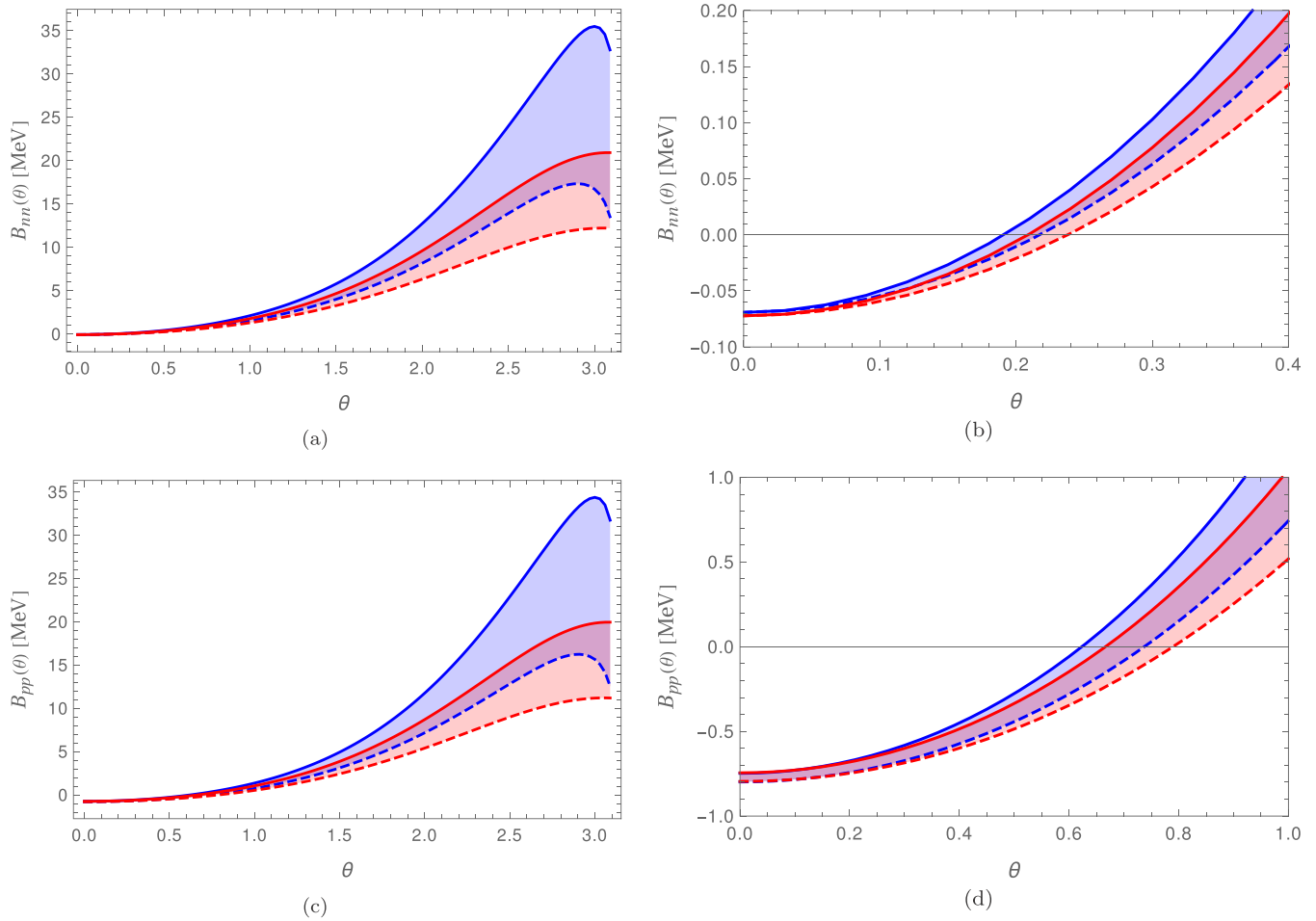


FIG. 7. The binding energies of the dineutron [(a) and (b)] zoom into the region  $\theta \leq 0.4$  and of the diproton [(c) and (d)] zoom into the region  $\theta \leq 1$  for the full  $\theta$ -dependent OBE model. In each figure, the blue (upper) band represents the isospin symmetric case and the red (lower) band the case of broken isospin symmetry. A band is spanned by a solid line based on parameter set I, Eq. (3.12), and a dashed line based on parameter set II, Eq. (3.13).

### C. Spin-singlet channel

The same analysis can be repeated for the dineutron with results shown in Figs. 7(a) and 7(b). Using Eqs. (3.6)–(3.9), one sees that the OPE and the  $\sigma$  exchange potentials are exactly the same for both deuteron and dineutron, i.e., with  $S = 1$  and  $I = 0$  (deuteron), and with  $S = 0$  and  $I = 1$  (dineutron). The vector exchange potentials on the other hand change in terms of the strength, but not regarding the overall sign: the  $\rho$  exchange potential is still attractive, but weakened by about 50%, whereas the  $\omega$  exchange potential is still repulsive, but weakened by about 1/3. The dineutron OBE potential is thus slightly less attractive in comparison with the deuteron OBE potential, so the dineutron fails to be bound, as in the real world. However, anything that happened to the deuteron OBE potential when sending  $\theta \rightarrow \pi$ , this also happens to the dineutron potential, i.e., the most decisive effects come from the  $\sigma$  exchange potential, which is getting stronger (while the increase of the  $\rho$  exchange attraction and the increase of the  $\omega$  exchange repulsion roughly neutralize), so the dineutron becomes bound. From Fig. 7(b) one sees that this happens already for  $\theta \simeq 0.18$ – $0.24$ .

The overall  $\theta$ -dependence of the dineutron’s binding energy is the same as for the deuteron. Note that while the binding energy of the dineutron steadily increases, it remains smaller than the binding energy of the deuteron.

We note that a bound dineutron is also found in lattice QCD calculations with pion masses larger than the physical one, see Refs. [67–70], which span pion masses from 300 to 510 MeV. The central binding energies in these works span the range from 7 to 13 MeV, similar to what we find at  $\theta = 1 - 2$ .

We end with a short discussion of the diproton with  $S = 0$  and  $I = 1$ . Referring to isospin symmetry, the only difference between the  $nm$  and the  $pp$  systems is the repulsive Coulomb interaction in the latter case:

$$V_C(r) = \frac{e^2}{r}, \tag{3.17}$$

with  $e$  the elementary charge. Adding this to our OBE potential Eq. (3.10), we find a constant shift of  $-0.67$  and  $-0.72$  MeV for sets I and II, respectively, compared to the dineutron case as shown in Figs. 7(c) and 7(d). The only visible effect of this is that the crossover point from the unbound to the bound case now happens at  $\theta \simeq 0.6 - 0.8$  [Fig. 7(d)].

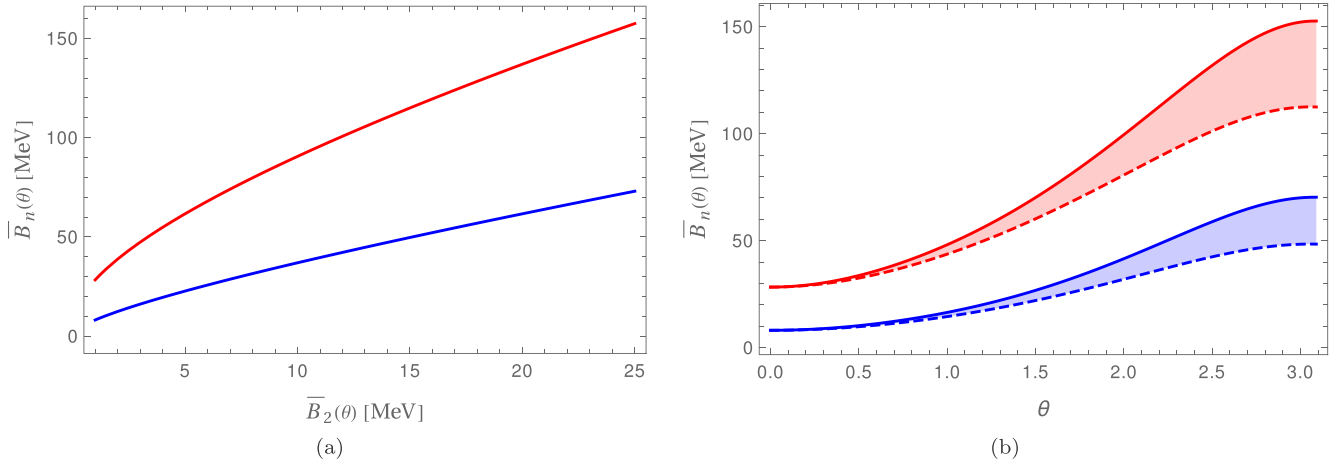


FIG. 8. (a) The SU(4)-averaged binding energy of the three- and four-nucleon systems  $\bar{B}_n(\theta)$  versus the SU(4)-averaged binding energy of the two-nucleon system,  $\bar{B}_2(\theta)$ . Blue (lower) line:  $n = 3$ . Red (upper) line:  $n = 4$ . (b)  $\bar{B}_n(\theta)$  versus  $\theta$ , taking isospin breaking effects into account, for parameter set I (solid lines), and parameter set II (dashed lines). Blue (lower) band:  $n = 3$ . Red (upper) band:  $n = 4$ .

#### IV. MORE THAN TWO NUCLEONS

##### A. Three and four nucleons

We have seen that the nucleon-nucleon interaction becomes more attractive as  $\theta$  increases. This is predominantly due to the decrease in the  $\sigma$  meson mass. Since the  $\sigma$  meson is a scalar particle with zero isospin, the increased attraction is approximately the same in the spin-singlet and spin-triplet channels. This is a realization of Wigner's SU(4) symmetry [71]. Wigner's SU(4) symmetry is an approximate symmetry of low-energy nuclear physics where the four spin and isospin degrees of freedom are four components of an SU(4) multiplet.

In the SU(4) limit where the spin-singlet and spin-triplet scattering lengths are large and equal, the properties of light nuclei with up to four nucleons follow the same universal behavior that describes attractive bosons at large scattering length [72–76]. We can use this information to determine the  $\theta$ -dependent binding energies of  ${}^3\text{H}$ ,  ${}^3\text{He}$ , and  ${}^4\text{He}$ . In order to perform this analysis, we first average over nuclear states which become degenerate in the SU(4) limit. For the  $A = 2$  system, we average over the physical deuteron and spin-singlet channel to arrive at an average binding energy of  $\bar{B}_2 \simeq 1$  MeV. For the  $A = 3$  system, we average over the physical  ${}^3\text{H}$  and  ${}^3\text{He}$  systems for an average binding energy of  $\bar{B}_3 = 8.1$  MeV. For the  $A = 4$  system, we take the physical  ${}^4\text{He}$  binding energy,  $\bar{B}_4 = 28.3$  MeV.

In order to extend these binding energies to nonzero  $\theta$ , we use the numerical results from a study of bosonic clusters at large scattering length [77]. In particular, we use an empirical observation from Fig. 7 of Ref. [77] that

$$[\bar{B}_n/B]^{1/4} - [\bar{B}_2/B]^{1/4} \quad (4.1)$$

remains approximate constant for positive scattering length  $a > 0$ , where  $B$  is a binding energy scale set by a combination of the range of the interaction and particle mass. Conveniently, the value of  $B$  is approximately equal to the value of  $\bar{B}_4$  at infinite scattering length. We use these empirical observations to determine  $\bar{B}_3(\theta)$  and  $\bar{B}_4(\theta)$  in terms of  $\bar{B}_2(\theta)$  using the

approximate relation

$$\begin{aligned} & [\bar{B}_n(\theta)/\bar{B}_4(0)]^{1/4} - [\bar{B}_2(\theta)/\bar{B}_4(0)]^{1/4} \\ &= [\bar{B}_n(0)/\bar{B}_4(0)]^{1/4} - [\bar{B}_2(0)/\bar{B}_4(0)]^{1/4}. \end{aligned} \quad (4.2)$$

In Fig. 8(a), we show the SU(4)-averaged binding energy of the three- and four-nucleon systems,  $\bar{B}_3(\theta)$  and  $\bar{B}_4(\theta)$ , versus the SU(4)-averaged binding energy of the two-nucleon system,  $\bar{B}_2(\theta)$ , and in Fig. 8(b) directly as a function of  $\theta$ . Our results are similar to those obtained in Ref. [78], which were computed using hyperspherical harmonics and auxiliary-field diffusion Monte Carlo. We should also mention that we find no evidence that varying theta will produce more exotic states of three or four nucleons such as a bound trineutron or tetra-neutron.

##### B. More than four nucleons

In Ref. [79], the authors noted that the strength of the  ${}^4\text{He}$ - ${}^4\text{He}$  interaction is controlled by the strength and range of the SU(4)-invariant local nucleon-nucleon interaction. By local we mean an interaction that is velocity independent. We have noted that as  $\theta$  increases, the range and strength of the SU(4)-invariant local nucleon-nucleon interaction increases due to the  $\sigma$  exchange contribution. We have already observed the increase in the binding energies of the two-, three-, and four-nucleon systems. As discussed in Ref. [79], the increase in the range of the local interaction will also cause alpha-like nuclei to become more bound. This is discussed further in Secs. V and VI B.

Across the nuclear chart, the binding energy per nucleon will increase with  $\theta$ , and the relative importance of the Coulomb interaction will decrease. As a result, the density of nucleons at nuclear saturation will also rise. Given the increase in the neutron-proton mass difference and decreased importance of the Coulomb interaction, the line of nuclear stability will shift towards nuclei with equal numbers of neutrons and protons and extend to larger nuclei.



### V. BIG BANG NUCLEOSYNTHESIS

In the early universe the temperature,  $T$ , is high enough to keep neutrons and protons in thermal equilibrium through the weak interactions

$$\begin{aligned} n + e^+ &\leftrightarrow p + \bar{\nu}_e, \\ n + \nu_e &\leftrightarrow p + e^-, \\ n &\leftrightarrow p + e^- + \bar{\nu}_e. \end{aligned} \quad (5.1)$$

The weak interaction rates scale as  $T^5$  and can be compared with the expansion rate of the Universe, given by the Hubble parameter,  $H \propto T^2$  in a radiation dominated Universe. As the temperature drops, the weak rates freeze-out, i.e., they fall out of equilibrium when they drop below the Hubble rate. In standard BBN, this occurs at a temperature,  $T_f \simeq 0.84$  MeV. In equilibrium, the ratio of the number densities of neutrons to protons follow the Boltzmann distribution

$$\frac{n}{p} \equiv \frac{n_n}{n_p} \simeq \exp\left[-\frac{\Delta m_N}{T}\right]. \quad (5.2)$$

At freeze-out, this ratio is about  $1/4.7$ . The neutron-to-proton ratio is particularly important, as it is the primary factor determining the  ${}^4\text{He}$  abundance. The  ${}^4\text{He}$  mass fraction,  $Y$ , can be written as

$$Y = 2X_n \equiv \frac{2(n/p)}{1 + (n/p)}, \quad (5.3)$$

and its observed value is  $Y = 0.2449 \pm 0.0040$  [80]. Further,  $X_n$  is the neutron fraction. A change in  $\theta$ , will therefore invariably affect the  ${}^4\text{He}$  abundance, primarily through the change in  $\Delta m_N$ . While the change in  $\theta$  and  $\Delta m_N$  does induce a change in  $T_f$ , this is minor ( $<10\%$  in  $T_f$ ) and we neglect it here.

The helium abundance, however, is not determined by  $(n/p)$  at freeze-out, but rather by the ratio at the time BBN begins. At the onset of BBN, deuterons are produced in the forward reaction

$$n + p \leftrightarrow d + \gamma. \quad (5.4)$$

However, initially (even though  $T < B_d$ ), deuteron is photo-disintegrated by the backward reaction at temperatures  $T_d \gtrsim 0.1$  MeV. This delay, often called the deuteron bottleneck, is caused by the large excess of photons-to-baryons (or the smallness of  $\eta_B$ ), and allows time for some fraction of the free neutrons to decay. A rough estimate of the temperature at which deuteron starts to form is

$$T_d \sim -\frac{B_d(\theta)}{\ln \eta_B} \quad (5.5)$$

which for  $\theta = 0$  yields  $T_d \sim 0.1$  MeV. A more accurate evaluation would find  $T_d \approx 0.064$  MeV. Below this temperature, the photo-disintegration processes become negligible and nucleosynthesis begins.

A change in the starting time of BBN changes the  $(n/p)$  at freeze-out or more accurately the neutron fraction,  $X_n$ , at freeze-out by

$$X_n(T_d) = X_n(T_f)e^{-t_d/\tau_n}, \quad (5.6)$$

where  $t_d$  is the age of the Universe corresponding to the temperature,  $T_d$ . As noted earlier,  $\Gamma_n \propto (\Delta m_N)^5$ , and in a

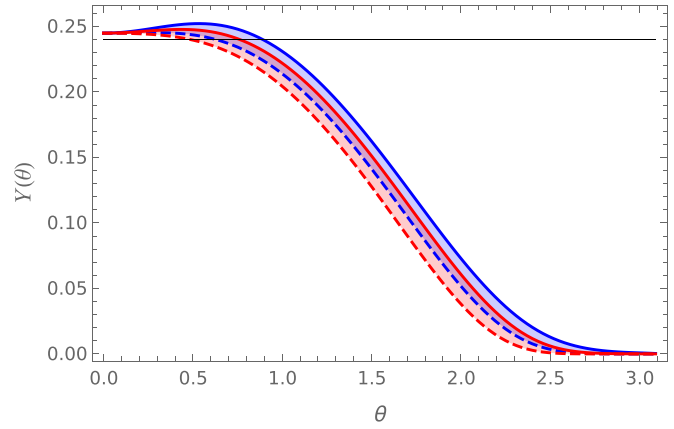


FIG. 9. The Helium mass fraction,  $Y$ , as a function of  $\theta$  in the isospin symmetric case (blue upper band) and in the case of broken isospin symmetry (red lower band) for parameter set I, Eq. (3.12) (solid lines) and parameter set II, Eq. (3.13) (dashed lines).

radiation dominated Universe,  $t \propto T^{-2}$ , so that from (5.5),  $t_d \propto B_d^{-2}$ . Thus using the dependencies of  $\Delta m_N$ ,  $\tau_n$ , and  $B_d$  on  $\theta$ , we can calculate  $Y(\theta)$  as shown in Fig. 9. Note that to produce Fig. 9 we have used the numerical values of  $\Gamma_n$  and  $B_d$  as in Figs. 4 and 6, rather than the analytic approximations.

As one can see in the figure, the Helium mass fraction is relatively flat for  $\theta \lesssim 1$ . This is due to competing effects in determining  $Y$ . As we saw in Fig. 2(b), the neutron-proton mass difference increases with  $\theta$ . This strongly suppresses the neutron-to-proton ratio, as seen in Eq. (5.2). Furthermore, because  $\Gamma_n \propto (\Delta m_N)^5$ , an even stronger suppression in  $Y$  occurs due to the increased neutron decay rate as seen in Eq. (5.6). However these decreases are largely canceled at low  $\theta$  by the increase in  $B_d$ , which causes BBN to begin earlier, leaving less time for neutron decay. In fact, for set I parameters, at low  $\theta$  this is the dominant change in  $Y$  and causes an increase in the Helium abundance. The maxima occur at  $\theta = 0.42(0.54)$  and  $Y = 0.248(0.252)$  for broken (unbroken) isospin symmetry. Requiring  $Y > 0.24$ , sets upper limits on  $\theta$  of roughly 0.77 (0.50) for broken isospin, and 0.89 (0.61) for unbroken isospin for parameter sets I (II), respectively. For larger values of  $\theta$ , the Helium abundance will drop below the observationally inferred limit,<sup>3</sup> however, as we note earlier, it is not clear that a Universe with primordial Helium and  $Y < 0.05$  would prevent the formation of life and therefore can not be excluded anthropically. We also note that an increase in  $\theta$  and an increased  $B_d$  will lead to an increase in the BBN value for D/H [31] which is now very tightly constrained by observation  $D/H = 2.53 \pm 0.03$  [81].

An interesting subtlety occurs in the case of unbroken isospin symmetry for parameter set I. As one can see in Fig. 6, the deuteron binding energy increases above  $\sim 30$  MeV, when  $\theta \gtrsim 2.4$ . In this case, there is effectively no deuteron bottleneck, as the backward reaction in (5.5) shuts off before

<sup>3</sup>While we have not run a nucleosynthetic chain in a numerical BBN analysis, the analytic approximation for  $Y$  is quite good. For  $\theta = 0$ , we have  $Y = 0.2467$ , while the current result from a full BBN analysis is  $Y = 0.24696$  [42].

weak decoupling. The Helium abundance, however, is highly suppressed due to the large value of  $\Delta m_N \gtrsim 3.5$  MeV and  $Y \lesssim 0.05$ .

As described above, the other two potentially bound dimers, the dineutron and the diproton, become bound at  $\theta \simeq 0.2$  and  $\theta \simeq 0.7$ , respectively. Variations in the binding energy of the dineutron is expected to have little effect on the primordial abundances provided its absolute value remains smaller than the deuteron's binding energy [29,82,83]. Considering that, in this work the variations on the binding energy of the deuteron are only of a few percent, we do not expect any important role played by the binding energy of the dineutron in the calculations. For large  $\theta$ , although diprotons are bound, their binding energy remains below that of deuteron and it was argued that diproton production freezes-out before the diproton bottleneck is broken [83,84].

Before concluding this section, we consider the possible impact of changes in the binding energy of unstable nuclei. In Ref. [30], changes in the nuclear part of the nucleon-nucleon potential were parameterized as

$$V_N(\mathbf{r}_{ij}) = (1 + \delta_{NN})V_N^0(\mathbf{r}_{ij}), \quad (5.7)$$

where  $V_N^0(\mathbf{r}_{ij})$  is the nucleon-nucleon potential based on the Minnesota force adapted to low mass systems [85]. The binding energy of  ${}^8\text{Be}$ , was found to be [30]

$$B_8 = (-0.09184 + 12.208\delta_{NN}) \text{ MeV} \quad (5.8)$$

indicating that  ${}^8\text{Be}$  becomes bound when  $\delta_{NN} \geq 0.00752$ .<sup>4</sup> The binding energy of deuteron is also affected by a change in the nucleon-nucleon potential

$$B_d(\theta) = (1 + 5.716\delta_{NN}(\theta))B_d(0), \quad (5.9)$$

where we have implicitly here made  $\theta$  the origin of this change. From these expressions, we estimate that  ${}^8\text{Be}$  becomes bound when  $B_d(\theta) = 2.32$  MeV or when  $\theta$  is 0.21 (0.23) for broken isospin, and 0.19 (0.22) for unbroken isospin for parameter sets I (II), respectively.

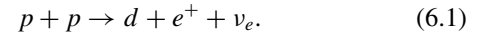
For stable  ${}^8\text{Be}$ , it may be possible in principle that BBN produce elements beyond  ${}^7\text{Li}$ . As we discuss further in the next section, changes in the nuclear potential strongly affects the triple  $\alpha$  process and the production of carbon and oxygen in stars [30]. In the context of BBN, stable  ${}^8\text{Be}$  increases the importance of two reactions  ${}^4\text{He}(\alpha, \gamma){}^8\text{Be}$  and  ${}^8\text{Be}(\alpha, \gamma){}^{12}\text{C}$ . Nevertheless, the detailed study in [31], found that while some  ${}^8\text{Be}$  is produced in BBN (with a mass fraction of  $10^{-16}$  for  $\delta_{NN} = 0.0116$ ), no enhancement of carbon occurs as the temperature and density in the BBN environment is substantially below that in stars and the production rates are inefficient.

<sup>4</sup>  ${}^5\text{He}$  and  ${}^5\text{Li}$  are unbound by 0.798 and 1.69 MeV, respectively, i.e., roughly an order of magnitude more than  ${}^5\text{Be}$  requiring a very substantial change in  $\delta_{NN}$  and we do not consider this possibility here.

## VI. STELLAR NUCLEOSYNTHESIS

### A. Hydrogen burning

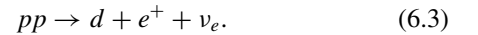
The effects of nonzero  $\theta$  will also be manifest in stellar nucleosynthesis. We first consider main sequence stars undergoing hydrogen burning. The first step of hydrogen burning is proton-proton fusion,



For  $\theta \lesssim 0.5$ , proton-proton fusion is not significantly altered from how it occurs in the physical Universe. However for  $\theta \gtrsim 0.7$ , the diproton becomes bound and the first step in hydrogen burning can proceed many orders of magnitude faster via radiative capture,



The diproton can then subsequently decay via the weak interactions to a deuteron,



We note that while the neutron-proton mass difference grows with  $\theta$ , the diproton still has a higher mass than the deuteron due to the larger binding energy of the deuteron.

Initially it was thought the rapid processing of protons to diprotons would lead to stars with extremely short lifetimes, so short so as to prevent the evolution of life on planets. However, stellar structure compensates, and burning occurs at lower temperatures and densities [84,96] and though the stars would be different, it is not clear that there is an anthropic argument against such stars.

### B. Constraints on $\theta$ from the anthropic principle

The anthropic principle can constrain  $\theta$  if changes in  $\theta$  result in a departure of normal stellar evolution so great that planetary life would not occur. Therefore we could at minimum require that (a) enough metals (in the astronomical sense) are available, and that (b) the lifetime of stars with higher metallicity (thus allowing for rocky planets with potentially living beings) is long enough that intelligent life can evolve. Perhaps two of the most important elements for the production of life as we know it are carbon and oxygen.

There have been many studies relating the sensitivity of carbon production to fundamental physics in relation to the anthropic principle [23,24,26,86–92]. The production of  ${}^{12}\text{C}$  in stars requires a triple fine tuning: (i) the decay lifetime of  ${}^8\text{Be}$ , is relatively long, and is of order  $10^{-16}$  s, which is four orders of magnitude longer than the scattering time for two  $\alpha$  particles, (ii) there must exist an excited state of carbon which lies just above the energy of  ${}^8\text{Be} + \alpha$  and (iii) the energy level of  ${}^{16}\text{O}$  which sits at 7.1197 MeV must be nonresonant and below the energy of  ${}^{12}\text{C} + \alpha$ , at 7.1616 MeV, so that most of the produced carbon is not destroyed by further stellar processing. It is well known of course, that the existence of the excited state of  ${}^{12}\text{C}$  was predicted by Hoyle [93]. Any change in fundamental physics which affects the position of the Hoyle resonance, could severely affect the production of carbon and oxygen and ultimately the existence of life.

We saw that it is perhaps not possible to place anthropic bounds on  $\theta$  from BBN, as it is hard to see why a universe with

a paucity of Helium would prevent star formation or stellar processing. It is however possible to set some constraints on  $\theta$  based on its effect on the triple  $\alpha$  process leading to carbon production in stars. In addition to the change in the  ${}^8\text{Be}$  binding energy given in Eq. (5.8), changes in  $\theta$  and thus changes in the nucleon-nucleon potential,  $\delta_{NN}$ , shift the energy level of the Hoyle resonance [30],

$$E_R = (0.2876 - 20.412\delta_{NN}) \text{ MeV}, \quad (6.4)$$

where the resonant energy is given with respect to the  ${}^8\text{Be} + \alpha$  threshold of 7.367 MeV. In standard stellar evolutionary models for massive stars, most  ${}^{12}\text{C}$  is produced during the He burning phase. When the temperature becomes high enough, the  ${}^{12}\text{C}(\alpha, \gamma){}^{16}\text{O}$  reaction begins and  ${}^{12}\text{C}$  is processed to  ${}^{16}\text{O}$ . Massive stars end their He burning phases with a mixture of C and O. When  $\delta_{NN} > 0$ , as would be expected for  $\theta \neq 0$ ,  $E_R$  is reduced, and the production of carbon becomes more efficient at a lower temperature. The burning of carbon to oxygen does not occur and stars end their Helium burning phases with a core of almost pure carbon.

If oxygen is not present after He burning, there is little chance to subsequently produce it. Though some oxygen is produced during carbon burning, the oxygen abundance in this phase of stellar evolution is reduced as oxygen is processed to Ne through  $\alpha$  capture. The analysis of Ref. [30] was based on stellar evolution models [94] of 15 and 60  $M_\odot$ , zero metallicity stars and found that for  $\delta_{NN} \geq 0.3\%$ , negligible amounts of oxygen survive the Helium burning phase. Thus an upper limit of  $\delta_{NN} < 0.002$  was set which corresponds to  $B_d < 2.25$  MeV. This is a rather tight bound and corresponds to upper limits on  $\theta$  of 0.11 (0.11) for broken isospin, and 0.11 (0.12) for unbroken isospin for parameter sets I (II), respectively. As shown above, the dineutron and the diproton remain unbound for such values of  $\theta$ , so that a universe with  $0 < \theta \lesssim 0.1$  will most probably look (almost) the same as a universe with  $\theta = 0$ .

## VII. SUMMARY AND CONCLUSIONS

Let us summarize the pertinent results of our investigation for  $0 < \theta < \pi$ .

(1) As  $\theta$  is increased, the deuteron is more strongly bound than in our world. This means that for  $\theta$  of the order one, there is much less fine-tuning than for  $\theta = 0$ . Also, in the case of isospin symmetry, the values for the binding energy as  $\theta$  approaches  $\pi$  are compatible with calculations for the chiral limit.

(2) The dineutron as well as the diproton are bound for  $\theta \gtrsim 0.2$  and  $\theta \gtrsim 0.7$ , respectively. A bound diproton has often been considered a disaster for the nucleosynthesis as we know it [95], but recent stellar calculations show that this might not be the case, see Refs. [83,84,96].

(3) Using Wigner's SU(4) symmetry and earlier results on systems with large scattering length, we have estimated the SU(4)-averaged binding energies of the three- and four-nucleon systems and found that these increase with increasing  $\theta$  or with the deuteron binding energy.

(4) In general, we have found that nuclear binding energies are quite significantly altered when  $\theta = \mathcal{O}(1)$ . While BBN would proceed, perhaps producing far less helium and more

deuterium, changes in the deuteron binding energy would not prevent the formation of stars and eventually life. Even a stable diproton can not be excluded on this basis as stars would continue to burn Hydrogen at lower temperatures. On the other hand, changes in the binding energy of  ${}^8\text{Be}$  and the resonant energy of the Hoyle state, would affect the triple  $\alpha$  reaction rate and lead to a world lacking in  ${}^{16}\text{O}$ .

(5) Applying the even stronger constraint not to upset the world as we enjoy it, we derived that  $\theta$  must be  $\lesssim 0.1$  in order to approximately recover the real nuclear reaction rates. In this case, the deviation of the neutron-proton mass difference to the real world value is less than 1% and both the diproton and the dineutron still fail to be bound.

## ACKNOWLEDGMENTS

M.S. is grateful to Alexey Cherman and Maxim Pospelov for useful discussions. U.G.M. thanks Karlheinz Langanke, Maxim Mai, and Andreas Wirzba for useful discussions. This work was supported by DFG and NSFC through funds provided to the Sino-German CRC 110 ‘‘Symmetries and the Emergence of Structure in QCD’’ (NSFC Grant No. 11621131001, DFG Grant No. TRR110). The work of U.G.M. was supported in part by VolkswagenStiftung DE (Grant No. 93562) and by the Chinese Academy of Sciences (CN) President’s International Fellowship Initiative (PIFI) (Grant No. 2018DM0034). The work of K.O. and M.S. is supported in part by U.S. Department of Energy (Grant No. DE-SC0011842) and the work of D.L. is supported in part by the U.S. Department of Energy (Grant No. DE-SC0018638) and the NUClear Computational Low-Energy Initiative (NUCLEI) SciDAC project.

## APPENDIX: $\theta$ -DEPENDENCE OF THE NEUTRON-PROTON MASS DIFFERENCE

The strong contribution to the proton-neutron mass difference can be derived from the NLO  $\pi N$  Lagrangian [54]

$$\mathcal{L}_{\pi N}^{\Delta m_N} = \bar{N} c_5 \left( \chi_+ - \frac{1}{2} \langle \chi_+ \rangle \right) N, \quad (A.1)$$

where  $c_5$  is a LEC,  $N = (p, n)^T$  contains the nucleon fields,  $\langle \dots \rangle$  denotes the trace in flavor space, and

$$\chi_+ = u^\dagger \chi_\theta u^\dagger + u \chi_\theta^\dagger u. \quad (A.2)$$

For the determination of the mass difference,  $U = u^2$ , which contains the pseudo-Nambu-Goldstone bosons of SU(2) chiral perturbation theory, only needs to be expanded up to its leading order constant term. In particular, in a  $\theta$ -vacuum  $U$  is given by the vacuum alignment  $U_0$ . For  $\chi_\theta = 2B\mathcal{M} \exp(i\theta/2)$ , with  $\mathcal{M} = \text{diag}\{m_u, m_d\}$  the quark mass matrix, we use the following parametrization of the vacuum alignment:

$$U_0 = \text{diag}\{e^{i\varphi}, e^{-i\varphi}\}. \quad (A.3)$$

Minimizing the vacuum energy density in SU(2) chiral perturbation theory (or equivalently removing the tree-level tadpole term of the neutral pion), one finds [48]

$$\tan \varphi = -\varepsilon \tan \frac{\theta}{2}, \quad (A.4)$$

or

$$\sin \varphi = \frac{-\varepsilon \tan \frac{\theta}{2}}{\sqrt{1 + \varepsilon^2 \tan^2 \frac{\theta}{2}}} = \frac{-\varepsilon M_\pi^2 \sin \frac{\theta}{2}}{M_\pi^2(\theta)}, \quad (\text{A.5})$$

$$\cos \varphi = \frac{1}{\sqrt{1 + \varepsilon^2 \tan^2 \frac{\theta}{2}}} = \frac{M_\pi^2 \cos \frac{\theta}{2}}{M_\pi^2(\theta)}, \quad (\text{A.6})$$

where we have used Eq. (2.1). With that, Eq. (A.1) becomes

$$\begin{aligned} \mathcal{L}_{\pi N}^{\Delta m_N} &= \bar{N} 4c_5 B_0 \frac{m_u \cos \left(\frac{\theta}{2} - \varphi\right) - m_d \cos \left(\frac{\theta}{2} + \varphi\right)}{2} \tau_3 N \\ &= \bar{N} 4c_5 B_0 \frac{M_\pi^2}{M_\pi^2(\theta)} \frac{m_u - m_d}{2} \tau_3 N, \end{aligned} \quad (\text{A.7})$$

which results in the strong contribution to the proton-neutron mass difference given in Eq. (2.10).

- 
- [1] B. Carter, Large number coincidences and the anthropic principle in cosmology, *IAU Symposium Confrontation of Cosmological Theories with Observational Data* (Reidel, Dordrecht, 1974), pp. 291–298.
- [2] S. Weinberg, Anthropic Bound on the Cosmological Constant, *Phys. Rev. Lett.* **59**, 2607 (1987).
- [3] For a comprehensive survey of the anthropic principle, see J. D. Barrow and F. J. Tipler, *The Anthropic Cosmological Principle* (Clarendon, Oxford, 1986).
- [4] L. Susskind, The Anthropic landscape of string theory, [arXiv:hep-th/0302219](https://arxiv.org/abs/hep-th/0302219) [hep-th].
- [5] J. Gegelia and U.-G. Meißner, Vacuum energy in the effective field theory of general relativity, *Phys. Rev. D* **100**, 046021 (2019).
- [6] C. Abel *et al.* [nEDM], Measurement of the Permanent Electric Dipole Moment of the Neutron, *Phys. Rev. Lett.* **124**, 081803 (2020).
- [7] T. Banks, M. Dine, and E. Gorbatov, Is there a string theory landscape? *J. High Energy Phys.* **08** (2004) 058.
- [8] J. F. Donoghue, Dynamics of M theory vacua, *Phys. Rev. D* **69**, 106012 (2004).
- [9] L. Ubaldi, Effects of theta on the deuteron binding energy and the triple-alpha process, *Phys. Rev. D* **81**, 025011 (2010).
- [10] N. Kaloper and J. Terning, Landscaping the Strong CP Problem, *J. High Energy Phys.* **03** (2019) 032.
- [11] M. Dine, L. Stephenson Haskins, L. Ubaldi, and D. Xu, Some Remarks on Anthropic Approaches to the Strong CP Problem, *J. High Energy Phys.* **05** (2018) 171.
- [12] J. Arakawa, A. Rajaraman, and T. M. P. Tait, Emergent Solution to the Strong CP Problem, *Phys. Rev. Lett.* **123**, 161602 (2019).
- [13] V. Flambaum and E. Shuryak, Limits on cosmological variation of strong interaction and quark masses from big bang nucleosynthesis, cosmic, laboratory and Oklo data, *Phys. Rev. D* **65**, 103503 (2002).
- [14] S. R. Beane and M. J. Savage, The Quark mass dependence of two nucleon systems, *Nucl. Phys. A* **717**, 91 (2003).
- [15] E. Epelbaum, U.-G. Meißner, and W. Gloeckle, Nuclear forces in the chiral limit, *Nucl. Phys. A* **714**, 535 (2003).
- [16] V. Dmitriev and V. Flambaum, Limits on cosmological variation of quark masses and strong interaction, *Phys. Rev. D* **67**, 063513 (2003).
- [17] V. Flambaum and E. Shuryak, Dependence of hadronic properties on quark masses and constraints on their cosmological variation, *Phys. Rev. D* **67**, 083507 (2003).
- [18] V. F. Dmitriev, V. Flambaum, and J. Webb, Cosmological variation of deuteron binding energy, strong interaction and quark masses from big bang nucleosynthesis, *Phys. Rev. D* **69**, 063506 (2004).
- [19] R. L. Jaffe, A. Jenkins, and I. Kimchi, Quark Masses: An Environmental Impact Statement, *Phys. Rev. D* **79**, 065014 (2009).
- [20] J. Berengut, V. Flambaum, and V. Dmitriev, Effect of quark-mass variation on big bang nucleosynthesis, *Phys. Lett. B* **683**, 114 (2010).
- [21] P. F. Bedaque, T. Luu, and L. Platter, Quark mass variation constraints from Big Bang nucleosynthesis, *Phys. Rev. C* **83**, 045803 (2011).
- [22] M. K. Cheoun, T. Kajino, M. Kusakabe, and G. J. Mathews, Time Dependent Quark Masses and Big Bang Nucleosynthesis Revisited, *Phys. Rev. D* **84**, 043001 (2011).
- [23] E. Epelbaum, H. Krebs, T. A. Lähde, D. Lee, and U.-G. Meißner, Viability of Carbon-Based Life as a Function of the Light Quark Mass, *Phys. Rev. Lett.* **110**, 112502 (2013).
- [24] E. Epelbaum, H. Krebs, T. A. Lähde, D. Lee, and U.-G. Meißner, Dependence of the triple-alpha process on the fundamental constants of nature, *Eur. Phys. J. A* **49**, 82 (2013).
- [25] J. Berengut, E. Epelbaum, V. Flambaum, C. Hanhart, U.-G. Meißner, J. Nebreda, and J. Pelaez, Varying the light quark mass: impact on the nuclear force and Big Bang nucleosynthesis, *Phys. Rev. D* **87**, 085018 (2013).
- [26] T. A. Lähde, U.-G. Meißner, and E. Epelbaum, An update on fine-tunings in the triple-alpha process, *Eur. Phys. J. A* **56**, 89 (2020).
- [27] B. A. Campbell and K. A. Olive, Nucleosynthesis and the time dependence of fundamental couplings, *Phys. Lett. B* **345**, 429 (1995).
- [28] J. P. Kneller and G. C. McLaughlin, BBN and Lambda(QCD), *Phys. Rev. D* **68**, 103508 (2003).
- [29] A. Coc, N. J. Nunes, K. A. Olive, J. P. Uzan, and E. Vangioni, Coupled Variations of Fundamental Couplings and Primordial Nucleosynthesis, *Phys. Rev. D* **76**, 023511 (2007).
- [30] S. Ekstrom, A. Coc, P. Descouvemont, G. Meynet, K. A. Olive, J. P. Uzan, and E. Vangioni, Effects of the variation of fundamental constants on Pop III stellar evolution, *Astron. Astrophys.* **514**, A62 (2010).
- [31] A. Coc, P. Descouvemont, K. A. Olive, J. P. Uzan, and E. Vangioni, The variation of fundamental constants and the role of A = 5 and A = 8 nuclei on primordial nucleosynthesis, *Phys. Rev. D* **86**, 043529 (2012).
- [32] K. A. Olive, M. Pospelov, Y. Z. Qian, A. Coc, M. Casse, and E. Vangioni-Flam, Constraints on the variations of the fundamental couplings, *Phys. Rev. D* **66**, 045022 (2002).
- [33] F. Luo, K. A. Olive, and J. P. Uzan, Gyromagnetic Factors and Atomic Clock Constraints on the Variation of Fundamental Constants, *Phys. Rev. D* **84**, 096004 (2011).
- [34] C. J. Hogan, Why the universe is just so, *Rev. Mod. Phys.* **72**, 1149 (2000).

- [35] L. A. Barnes, The fine-tuning of the universe for intelligent life, *Publ. Astron. Soc. Aust.* **29**, 529 (2012).
- [36] A. Schellekens, Life at the interface of particle physics and string theory, *Rev. Mod. Phys.* **85**, 1491 (2013).
- [37] U.-G. Meißner, Anthropic considerations in nuclear physics, *Sci. Bull.* **60**, 43 (2015).
- [38] F. C. Adams, The degree of fine-tuning in our universe—and others, *Phys. Rep.* **807**, 1 (2019).
- [39] V. Baluni, CP Violating Effects in QCD, *Phys. Rev. D* **19**, 2227 (1979).
- [40] F. K. Guo, R. Horsley, U. G. Meissner, Y. Nakamura, H. Perlt, P. Rakow, G. Schierholz, A. Schiller, and J. Zanotti, The Electric Dipole Moment of the Neutron from 2+1 Flavor Lattice QCD, *Phys. Rev. Lett.* **115**, 062001 (2015).
- [41] A. V. Smilga, QCD at theta similar to pi, *Phys. Rev. D* **59**, 114021 (1999).
- [42] B. D. Fields, K. A. Olive, T. H. Yeh, and C. Young, Big-bang nucleosynthesis after planck, *JCAP* **03**, 010 (2020).
- [43] G. Steigman and R. J. Scherrer, Is The Universal Matter - Antimatter Asymmetry Fine Tuned? [arXiv:1801.10059](https://arxiv.org/abs/1801.10059) [astro-ph.CO].
- [44] A. Sakharov, Violation of CP Invariance, C asymmetry, and baryon asymmetry of the universe, *Sov. Phys. Usp.* **34**, 392 (1991).
- [45] V. Kuzmin, M. Shaposhnikov, and I. Tkachev, Strong CP violation, electroweak baryogenesis, and axionic dark matter, *Phys. Rev. D* **45**, 466 (1992).
- [46] L. J. Hall, D. Pinner, and J. T. Ruderman, The Weak Scale from BBN, *J. High Energy Phys.* **12** (2014) 134.
- [47] H. Leutwyler and A. V. Smilga, Spectrum of Dirac operator and role of winding number in QCD, *Phys. Rev. D* **46**, 5607 (1992).
- [48] R. Brower, S. Chandrasekharan, J. W. Negele, and U. J. Wiese, QCD at fixed topology, *Phys. Lett. B* **560**, 64 (2003).
- [49] T. Fugleberg, I. E. Halperin, and A. Zhitnitsky, Domain walls and theta dependence in QCD with an effective Lagrangian approach, *Phys. Rev. D* **59**, 074023 (1999).
- [50] G. Colangelo, J. Gasser, and H. Leutwyler, The Quark Condensate from K(e4) Decays, *Phys. Rev. Lett.* **86**, 5008 (2001).
- [51] N. R. Acharya, F. K. Guo, M. Mai, and U.-G. Meißner,  $\theta$ -dependence of the lightest meson resonances in QCD, *Phys. Rev. D* **92**, 054023 (2015).
- [52] M. Hoferichter, J. Ruiz de Elvira, B. Kubis, and U.-G. Meißner, Roy-Steiner-equation analysis of pion-nucleon scattering, *Phys. Rep.* **625**, 1 (2016).
- [53] M. Hoferichter, J. Ruiz de Elvira, B. Kubis, and U.-G. Meißner, Matching Pion-Nucleon Roy-Steiner Equations to Chiral Perturbation Theory, *Phys. Rev. Lett.* **115**, 192301 (2015).
- [54] V. Bernard, N. Kaiser, and U.-G. Meißner, Chiral dynamics in nucleons and nuclei, *Int. J. Mod. Phys. E* **4**, 193 (1995).
- [55] N. Fettes, U.-G. Meißner, and S. Steininger, Pion - nucleon scattering in chiral perturbation theory. 1. Isospin symmetric case, *Nucl. Phys. A* **640**, 199 (1998).
- [56] V. Baru, C. Hanhart, M. Hoferichter, B. Kubis, A. Nogga, and D. Phillips, Precision calculation of threshold  $\pi^-d$  scattering,  $\pi$  N scattering lengths, and the GMO sum rule, *Nucl. Phys. A* **872**, 69 (2011).
- [57] J. Sakurai, Theory of strong interactions, *Annals Phys.* **11**, 1 (1960).
- [58] J. F. Donoghue, Sigma exchange in the nuclear force and effective field theory, *Phys. Lett. B* **643**, 165 (2006).
- [59] T. Damour and J. F. Donoghue, Constraints on the variability of quark masses from nuclear binding, *Phys. Rev. D* **78**, 014014 (2008).
- [60] E. Epelbaum, U.-G. Meißner, W. Gloeckle, and C. Elster, Resonance saturation for four nucleon operators, *Phys. Rev. C* **65**, 044001 (2002).
- [61] V. Bernard, N. Kaiser, and U.-G. Meißner, Aspects of chiral pion - nucleon physics, *Nucl. Phys. A* **615**, 483 (1997).
- [62] J. Gasser, H. Leutwyler, and A. Rusetsky, On the mass difference between proton and neutron, [arXiv:2003.13612](https://arxiv.org/abs/2003.13612) [hep-ph].
- [63] T. Vonk, Studies on the QCD  $\theta$ -vacuum in chiral perturbation theory, MSc. thesis, Bonn University, 2019.
- [64] E. Fermi, An attempt of a theory of beta radiation. 1., *Z. Phys.* **88**, 161 (1934).
- [65] T. E. O. Ericson and W. Weise, Pions and Nuclei, Int. Ser. Monogr. Phys. **74** (1988).
- [66] P. Mergell, U.-G. Meißner, and D. Drechsel, Dispersion theoretical analysis of the nucleon electromagnetic form-factors, *Nucl. Phys. A* **596**, 367 (1996).
- [67] S. Beane *et al.* [NPLQCD], The deuteron and exotic two-body bound states from lattice QCD, *Phys. Rev. D* **85**, 054511 (2012).
- [68] T. Yamazaki, K. i. Ishikawa, Y. Kuramashi, and A. Ukawa, Helium nuclei, deuteron and dineutron in 2+1 flavor lattice QCD, *Phys. Rev. D* **86**, 074514 (2012).
- [69] T. Yamazaki, K. i. Ishikawa, Y. Kuramashi, and A. Ukawa, Study of quark mass dependence of binding energy for light nuclei in 2+1 flavor lattice QCD, *Phys. Rev. D* **92**, 014501 (2015).
- [70] K. Orginos, A. Parreno, M. J. Savage, S. R. Beane, E. Chang, and W. Detmold, Two nucleon systems at  $m_\pi \sim 450\text{MeV}$  from lattice QCD, *Phys. Rev. D* **92**, 114512 (2015).
- [71] E. Wigner, On the consequences of the symmetry of the nuclear Hamiltonian on the spectroscopy of nuclei, *Phys. Rev.* **51**, 106 (1937).
- [72] P. F. Bedaque, H. Hammer, and U. van Kolck, Renormalization of the Three-Body System with Short Range Interactions, *Phys. Rev. Lett.* **82**, 463 (1999).
- [73] P. F. Bedaque, H. Hammer, and U. van Kolck, The Three boson system with short range interactions, *Nucl. Phys. A* **646**, 444 (1999).
- [74] P. F. Bedaque, H. Hammer, and U. van Kolck, Effective theory of the triton, *Nucl. Phys. A* **676**, 357 (2000).
- [75] L. Platter, H. Hammer, and U.-G. Meißner, The Four boson system with short range interactions, *Phys. Rev. A* **70**, 052101 (2004).
- [76] L. Platter, H. W. Hammer, and U.-G. Meißner, On the correlation between the binding energies of the triton and the alpha-particle, *Phys. Lett. B* **607**, 254 (2005).
- [77] M. Gattobigio, A. Kievsky, and M. Viviani, Energy spectra of small bosonic clusters having a large two-body scattering length, *Phys. Rev. A* **86**, 042513 (2012).
- [78] N. Barnea, L. Contessi, D. Gazit, F. Pederiva, and U. van Kolck, Effective Field Theory for Lattice Nuclei, *Phys. Rev. Lett.* **114**, 052501 (2015).
- [79] S. Elhatisari, N. Li, A. Rokash, J. M. Alarcon, D. Du, N. Klein, B. N. Lu, U.-G. Meißner, E. Epelbaum, H. Krebs, T. A. Lähde, D. Lee, and G. Rupak, Nuclear Binding Near a Quantum Phase Transition, *Phys. Rev. Lett.* **117**, 132501 (2016).

- [80] E. Aver, K. A. Olive, and E. D. Skillman, The effects of He I  $\lambda 10830$  on helium abundance determinations, *JCAP* **07** (2015) 011.
- [81] R. J. Cooke, M. Pettini, and C. C. Steidel, One percent determination of the primordial deuterium abundance, *Astrophys. J.* **855**, 102 (2018).
- [82] J. P. Kneller and G. C. McLaughlin, The Effect of bound dineutrons upon BBN, *Phys. Rev. D* **70**, 043512 (2004).
- [83] J. MacDonald and D. Mullan, Big bang nucleosynthesis: The strong force meets the weak anthropic principle, *Phys. Rev. D* **80**, 043507 (2009).
- [84] R. A. W. Bradford, The effect of hypothetical diproton stability on the universe, *J. Astrophys. Astron.* **30**, 119 (2009).
- [85] D. Thompson, M. Lemere, and Y. Tang, Systematic investigation of scattering problems with the resonating-group method, *Nucl. Phys. A* **286**, 53 (1977).
- [86] M. Livio, D. Hollowell, J. W. Truran, and A. Weiss, *Nature (London)* **340**, 281 (1989).
- [87] M. Fairbairn, carbon burning in supernovae and evolving physical constants, [arXiv:astro-ph/9910328](https://arxiv.org/abs/astro-ph/9910328) [astro-ph].
- [88] A. Csoto, H. Oberhummer, and H. Schlattl, Fine tuning the basic forces of nature through the triple alpha process in red giant stars, *Nucl. Phys. A* **688**, 560 (2001).
- [89] H. Oberhummer, A. Csoto, and H. Schlattl, Stellar production rates of carbon and its abundance in the universe, *Science* **289**, 88 (2000).
- [90] H. Schlattl, A. Heger, H. Oberhummer, T. Rauscher, and A. Csoto, Sensitivity of the c and o production on the 3-alpha rate, *Astrophys. Space Sci.* **291**, 27 (2004).
- [91] C. Tur, A. Heger, and S. M. Austin, Dependence of s-process nucleosynthesis in massive stars on triple-alpha and  $^{12}\text{C}(\alpha, \text{g})^{16}\text{O}$  reaction rate uncertainties, *Astrophys. J.* **702**, 1068 (2009).
- [92] L. Huang, F. C. Adams, and E. Grohs, Sensitivity of carbon and oxygen yields to the triple-alpha resonance in massive stars, *Astropart. Phys.* **105**, 13 (2019).
- [93] F. Hoyle, On nuclear reactions occurring in very hot stars. 1. the synthesis of elements from carbon to nickel, *Astrophys. J. Suppl.* **1**, 121 (1954).
- [94] S. Ekstrom, G. Meynet, C. Chiappini, R. Hirschi, and A. Maeder, Effects of rotation on the evolution of primordial stars, *Astron. Astrophys.* **489**, 685 (2008).
- [95] F. J. Dyson, Energy in the universe, *Sci. Am.* **225**, 50 (1971).
- [96] L. A. Barnes, Binding the diproton in stars: Anthropoc limits on the strength of gravity, *JCAP* **12** (2015) 050.